Journal of
Medicinal Chemistry

Article

A potent isoprenylcysteine carboxylmethyltransferase (ICMT) inhibitor improves survival in Ras-driven acute myeloid leukemia

Nagore I. Marin-Ramos, Moisés Balabasquer, Francisco J. Ortega-Nogales, Iván R. Torrecillas, Ana Gil-Ordoñez, Beatriz Marcos-Ramiro, Pedro Aguilar-Garrido, Ian Cushman, Antonio Romero, Francisco J. Medrano, Consuelo Gajate, Faustino Mollinedo, Mark R. Philips, Mercedes Campillo, Miguel Gallardo, Mar Martín-Fontecha, María L. López-Rodríguez, and Silvia Ortega-Gutierrez

J. Med. Chem., **Just Accepted Manuscript** • DOI: 10.1021/acs.jmedchem.9b00145 • Publication Date (Web): 10 Jun 2019

Just Accepted

is published by the American Chemical Society. 1155 Sixteenth Street N.W., Washington, DC 20036

A potent isoprenylcysteine carboxylmethyltransferase (ICMT) inhibitor improves survival in Ras-driven acute myeloid leukemia

Nagore I. Marín-Ramos,[1,2,#] Moisés Balabasquer,[1,#] Francisco J. Ortega-Nogales,[1,#] Iván R. Torrecillas,[3] Ana Gil-Ordóñez,[1] Beatriz Marcos-Ramiro,[1] Pedro Aguilar-Garrido,[4] Ian Cushman,[5] Antonio Romero,[6] Francisco J. Medrano,[6] Consuelo Gajate,[6] Faustino Mollinedo,[6] Mark R. Philips,[7] Mercedes Campillo,[3] Miguel Gallardo,[4] Mar Martín-Fontecha,[1] María L. López-Rodríguez[1,*] and Silvia Ortega-Gutiérrez[1,*]

[1]Departamento de Química Orgánica I, Facultad de Ciencias Químicas, Universidad Complutense de Madrid, E-28040 Madrid, Spain

[2]CEI Campus Moncloa, UCM-UPM and CSIC, E-28040 Madrid, Spain

[3]Laboratori de Medicina Computacional, Unitat de Bioestadística, Facultat de Medicina, Universitat Autònoma de Barcelona, E-08193 Bellaterra, Barcelona, Spain

[4]H12O-CNIO Haematological Malignancies Clinical Research Unit, Centro Nacional de Investigaciones Oncológicas (CNIO), E-28029 Madrid, Spain

[5]Department of Pharmacology and Cancer Biology, Duke University Medical Center, Durham, NC 27710, USA

[6]Centro de Investigaciones Biológicas, CSIC, E-28040 Madrid, Spain

[7]Perlmutter Cancer Center, New York University School of Medicine, New York, NY 10016, USA

[#]These authors contributed equally to this work

[*]Correspondence: mluzlr@ucm.es, siortega@ucm.es

ABSTRACT

Blockade of Ras activity by inhibiting its post-translational methylation catalysed by isoprenylcysteine carboxylmethyltransferase (ICMT) has been suggested as a promising antitumor strategy. However, the paucity of inhibitors has precluded the clinical validation of this approach. In this work we report a potent ICMT inhibitor, compound **3** [UCM-1336, IC_{50} = 2 μM], which is selective against the other enzymes involved in the post-translational modifications of Ras. Compound **3** significantly impairs the membrane association of the four Ras isoforms, leading to a decrease of Ras activity and to inhibition of Ras downstream signaling pathways. In addition, it induces cell death in a variety of Ras-mutated tumor cell lines and increases survival in an

in vivo model of acute myeloid leukemia. Because ICMT inhibition impairs the activity of the four Ras isoforms regardless of its activating mutation, compound **3** surmounts many of the common limitations of available Ras inhibitors described so far. In addition, these results validate ICMT as a valuable target for the treatment of Ras-driven tumors.

INTRODUCTION

Constitutively activated Ras is present in about one-third of the human cancers, including those among the most aggressive ones such as pancreatic, lung, or colon cancers or some leukemias. However, after several decades of continuous research efforts, Ras direct inhibition with small molecules still remains a current challenge.[1-7] Instead, interference with the enzymes involved in the post-translational modification of Ras could be an alternative, considering that in absence of any of its post-translational modifications Ras losses its capacity to promote tumor transformation.[8] Ras post-translational modification involves three consecutive steps: prenylation, catalysed by farnesyltransferase (FTase) or geranylgeranyltransferase (GGTase), proteolysis, mediated by the endoprotease Ras-converting enzyme 1 (Rce1), and final methylation of the carboxy terminal amino acid by the enzyme isoprenylcysteine carboxylmethyltransferase (ICMT). Though FTase has been the target of a variety of drug discovery programs, its inhibitors failed to show satisfactory activity in clinical trials, probably because of the alternative prenylation by GGTase. Consequently, more recent efforts have been dedicated to target the post-prenylation enzymes Rce1 and ICMT.[9] Whereas Rce1 inhibition has raised some toxicity concerns, ICMT blockade seems more promising given that its genetic inactivation blocks

Ras proper localization and activity,[10] ameliorates phenotypes of K-Ras-induced malignancies in vivo,[11] and is critical for malignant transformation and tumor maintenance by all Ras isoforms in humans.[12] These findings provide a compelling rationale for the development of ICMT inhibitors as a promising approach to anticancer drug development for treating challenging Ras-driven tumors. However, its clinical validation has been hampered by the lack of synthetic inhibitors and to date only one inhibitor, cysmethynil**13** (Figure 1A), has been thoroughly characterized. This compound effectively blocks the anchorage independent growth in a human colon cancer cell line**13** and impairs tumor progress in mice.[14, 15] However, its advancement towards clinical phases has been hampered by its limited potency in vitro in some cancer cell lines[14, 16] and in vivo models, where doses between 100 and 200 mg/kg are usually required to observe inhibition of tumor growth.[14, 15] Further efforts in the development of more efficacious ICMT inhibitors have led to the identification of several structural scaffolds able to inhibit in some extent ICMT,[17-20] including indole derivatives,[21, 22] some of them structurally similar to cysmethynil but with improved cellular antiproliferative activities,[16, 23] farnesyl cysteine analogs,[24-26] and a series of tetrahydropyrane derivatives, being one of these compounds the most potent ICMT inhibitor described to date, with a IC_{50} value of 1.3 nM.

However, this excellent in vitro value led only to a modest reduction in cell viability in different tumor cell lines.[27] In this context, new compounds able to block ICMT activity would be highly desirable. In this work we describe a new potent and selective ICMT inhibitor, compound **3**, which significantly impairs the membrane association of the four Ras isoforms, leading to a remarkable reduction in Ras activity, to the inhibition of the mitogen-activated protein kinase (MAPK) signaling pathway, and finally to cell death by autophagy and apoptosis. In addition, compound **3** significantly reduces cell viability in a variety of Ras-mutated tumor cell lines and, importantly, shows in vivo activity, as it increases survival in the Ras-driven model of acute myeloid leukemia at a dose of 25 mg/kg without causing any toxic side effect.

RESULTS AND DISCUSSION

Hit identification

In order to identify new ICMT inhibitors, we carried out a screening of our in-house library that led to the identification of compound **1** as an initial hit (Figure 1A). This compound blocked ICMT activity, albeit with moderate potency (25% inhibition of the ICMT activity at 50 μM), making necessary further optimization of the compound. As a first step in that direction, we decided to perform docking studies. For this, we built a homology model of the

human enzyme (h-ICMT) using as templates the *Methanosarcina acetivorans* ICMT (Ma-ICMT),[28] the only structure available when this work was started (Supporting Figure S1), and the recently disclosed *Tribolium castaneum* enzyme (Tc-ICMT),[29] the only eukaryotic ICMT described up to date (Supporting Figure S2). Analysis of the complexes between the Ma-ICMT derived h-ICMT with *N*-acetyl-*S*-farnesyl-L-cysteine (AFC), the minimal structural element recognized by ICMT (Supporting Figure S1, panel B), or with the inhibitor cysmethynil (Supporting Figure S1, panel C) showed the possibility of adding, in compound **1**, a hydrophobic tail to expand toward the membrane through the substrate tunnel, similarly to the farnesyl moiety of AFC or the octyl chain of cysmethynil. An analogous situation was observed in the models of the h-ICMT derived from Tc-ICMT in complex with cysmethynil (Figure 1B) or with AFC (Figure 1C), fact that prompted us to design and synthesize derivative **2** (Figure 2A). Remarkably, this compound displayed an enhanced capacity to inhibit ICMT activity (55% inhibition at 50 μM).

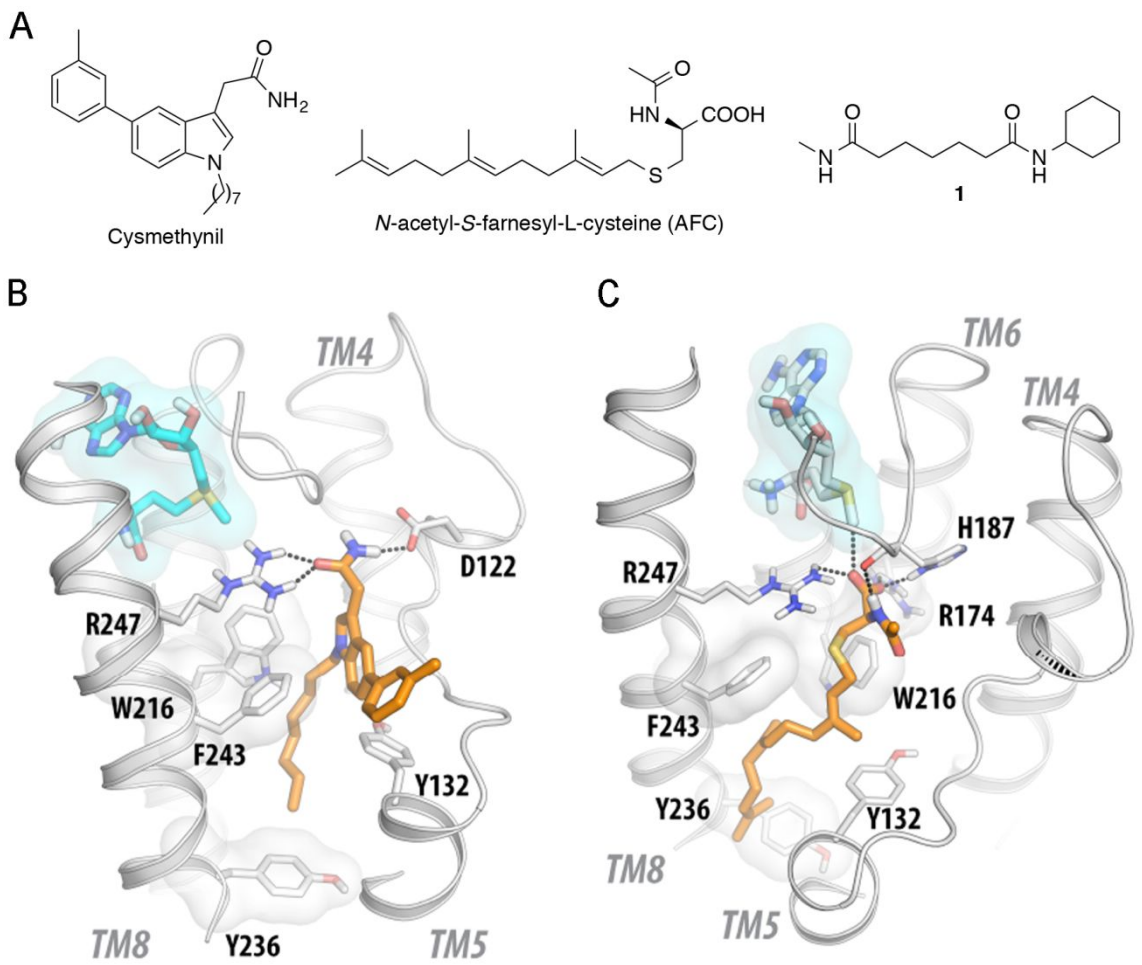

Figure 1. (A) Structures of cysmethynil, AFC, and compound **1**. (B) A Tc-ICMT-derived homology model of h-ICMT in complex with cysmethynil (orange) and *S*-adenosylmethionine (SAM) cofactor (cyan). The indol ring is positioned in front of Trp216, the amide group is located between Arg274 and Asp122, and the octyl tail expands towards Tyr236. (C) A Tc-ICMT-derived homology model of h-ICMT in complex with AFC (orange) and SAM cofactor (cyan). AFC positions the carboxyl group between conserved Arg174, His187, Arg247, Trp216 and the methyl group of SAM. The prenyl moiety expands between TM5 and TM8 helices towards Tyr236. Tc-ICMT PDB code: 5V7P.

A closer look to the interaction model between compound **2** and the protein (Figure 2A) highlighted the presence of a cluster of aromatic amino acids in the binding site formed by Trp216 of TM7 and Phe243 and Phe244 of TM8. Hence, it would be conceivable that the replacement of the methyl and cyclohexyl substituents of compound **2** by phenyl rings, able to establish π-π stacking interactions, allowed for an improvement of affinity towards the protein. Consequently, we designed compound **3**, which fitted perfectly in the model (Figure 2B). One phenyl ring can fill the pocket formed by Arg174 of TM6, Tyr213 and Trp216 of TM7 and Phe243 and Phe244 of TM8. The amide group is hydrogen bonding Arg247 of TM8 and the octyl chain of the ligand fills the lipid site. The other phenyl group is placed between the TM5-TM8 crevice, while the adjacent amide group is able to establish a hydrogen bond with Ser129 on the top of TM5 (Figure 2B). It is worthy to mention that the h-ICMT model based on the Tc-ICMT structure, as well as all the mutagenesis data published to date, confirm the conserved interactions of ICMT ligands with Arg247 below the cofactor binding site. Hence, compound **3** was synthesized and tested for ICMT activity, showing, to our delight, an excellent 93% enzyme activity inhibition at 50 μM and an IC_{50} value of 2 μM (see Supporting Figure S3 for a representative dose-response curve).

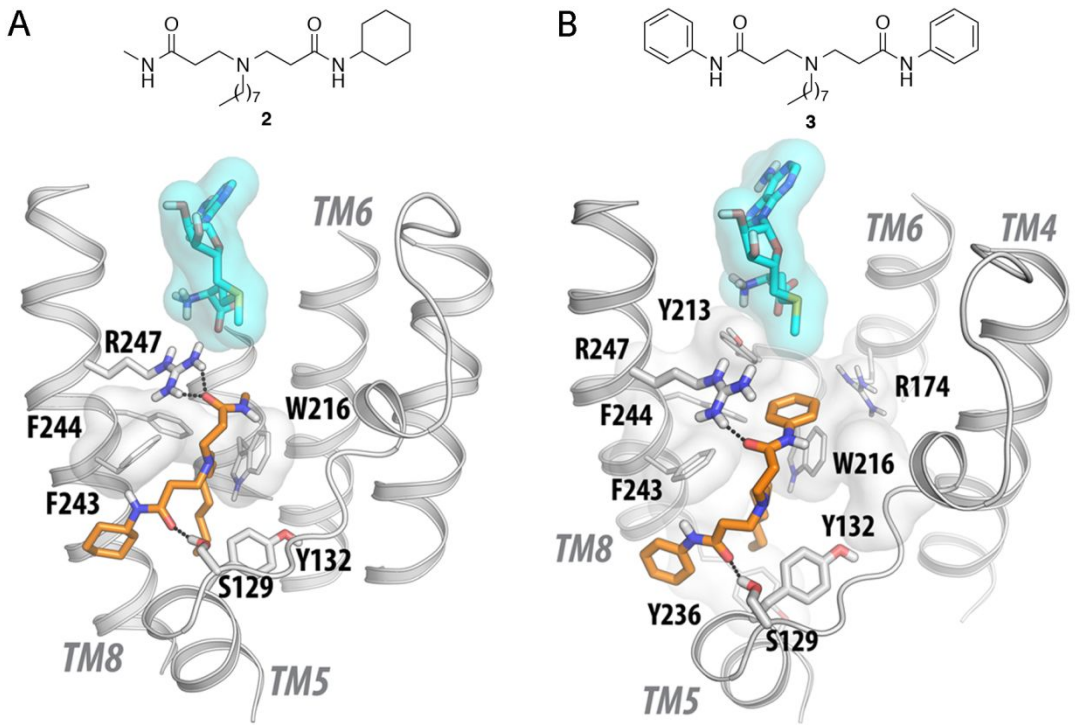

Figure 2. Tc-ICMT-derived homology models of h-ICMT in complex with compounds **2** and **3**. (A) Compound **2** (in orange) positions the octyl chain toward the membrane in a similar manner as the hydrophobic tail of cysmethynil and AFC. *S*-adenosylmethionine (SAM) cofactor is shown in cyan. (B) Extracellular view of the homology model of the h-ICMT in complex with compound **3** (orange) and SAM (cyan). Tc ICMT PDB code: 5V7P.

The importance of the structural elements suggested by the model was confirmed with the synthesis of several sets of compounds. In this regard, we verified that replacement of one or the two phenyl rings by non-aromatic moieties (cpds **4-10**, Figure 3) led to a decrease in activity (Figure 3 and Table 1). Also, we validated the importance of the *n*-octyl chain because its substitution by shorter or oxygen-containing chains (cpds **11-16**, Figure 3 and Table 2)

dramatically diminishes activity when compared to the 93% inhibition of compound **3**.

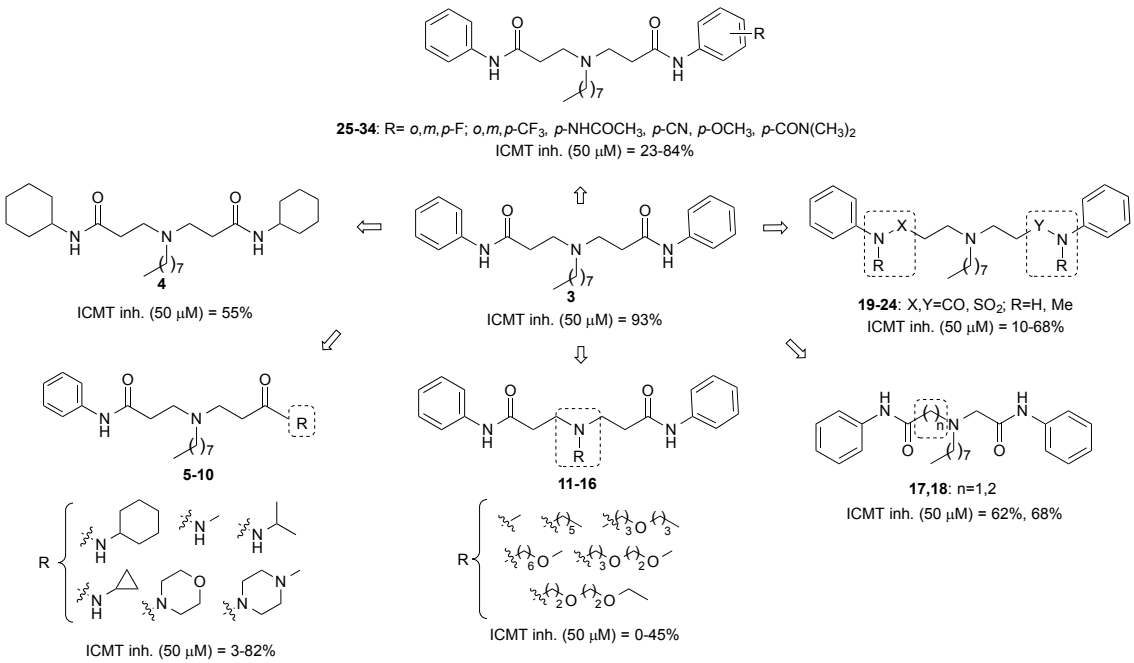

Figure 3. Synthesized compounds **3-34**.

Table 1. Inhibition of ICMT activity of synthesized compounds **5-10**

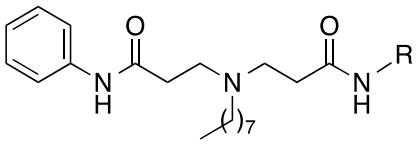

Cpd	R	ICMT inhibition (%)[a]	Cpd	R	ICMT inhibition (%)[a]
5	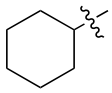	82±3 (12±3)[b]	**8**		48±6
6	$-CH_3$	30±5	**9**	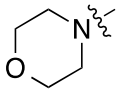	Inactive[c]

7		20±2	**10**	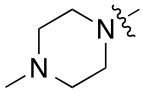	29±5

[a] The values are the mean±standard error of the mean (SEM) from two to three independent experiments performed in triplicate. ICMT inhibition values were determined at 50 μM. [b] IC_{50} values for ICMT inhibition are shown between parentheses. Data correspond to the mean±SEM from two independent experiments carried out in duplicate. [c] Compounds inhibiting less than 10% of the ICMT activity at 50 μM were considered inactive.

Table 2. Inhibition of ICMT activity of synthesized compounds **11-16**

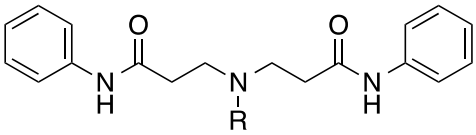

Cpd	R	ICMT inhibition (%)[a]	Cpd	R	ICMT inhibition (%)[a]
11	$-CH_3$	Inactive[b]	**14**	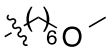	30±8
12		Inactive[b]	**15**	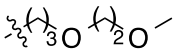	45±6
13	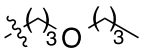	14±4	**16**	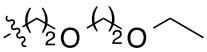	15±3

[a] The values are the mean±SEM from two to three independent experiments performed in triplicate. ICMT inhibition values were determined at 50 μM. [b] Compounds inhibiting less than 10% of the ICMT activity at 50 μM were considered inactive.

In addition, the adequate distance between the two carbonyl groups was confirmed with the synthesis of derivatives **17** and **18**, which also showed a decrease in activity (Figure 3 and Table 3). The exploration of different

hydrogen acceptor groups such as *N*-methyl amides and sulphonamides (cpds **19**-**24**, Figure 3 and Table 3) did not yield any enhancement in activity. Finally, we also studied whether the inhibitory capacity of the compound could be improved by the introduction of different substituents in the phenyl ring (cpds **25-34**, Figure 3). The obtained results suggest that only the introduction of small substituents in the *para* position keeps the ability to inhibit ICMT (Table 4) being the *p*-fluor derivative **27**, with 84% inhibition at 50 μM and an IC_{50} value of 3 μM the best inhibitor within this series. Although none of the synthesized analogues was able to improve the activity of inhibitor **3**, compounds **5** and **27** showed comparable values to derivative **3** in terms of ICMT inhibitory potency (maximal inhibition values between 82% and 93% at 50 μM). Accordingly, they were evaluated for their IC_{50} value at ICMT, for in vitro cellular activity, and for their ADME profile (Table 5). Taken together, these data showed that compound **3** not only exhibited the best value in terms of ICMT inhibition (93% of maximal activity and IC_{50} value of 2 μM vs 82% of maximal activity and 12 μM of compound **5** and 84% and 3 μM of compound **27**) but also the lowest clogP (4.1 for compound **3** vs 5.1 and 4.5 for derivatives **5** and **27**, respectively) and the highest cellular activity (IC_{50} value of 5 μM for compound **3**, whereas the IC_{50} values for compounds **5** and **27** were 29.1 and 13.7 μM, respectively). These results, together with the higher permeability (68% for compound **3** vs 50% and 54% for compounds **5** and **27**, respectively), stability in mouse serum

(171 min for compound **3** compared to 118 and 55 min for compounds **5** and **27**, respectively) and in human serum (>24 h), and the slightly lower human serum albumin (HSA) binding, prompted us to select compound **3** for an in-depth cellular and in vivo characterization aimed at validating ICMT as a target of interest for Ras inhibition. Towards this objective we sought to confirm that the inhibition of ICMT by compound **3** (i) delocalizes Ras from the membrane; (ii) inactivates Ras and its downstream signaling pathways; (iii) induces cell death in Ras-dependent tumor cell lines; and (iv) has in vivo efficacy in Ras-dependent tumors.

Table 3. Inhibition of ICMT activity of synthesized compounds **17-24**

Cpd		ICMT inhibition (%) [a]
17	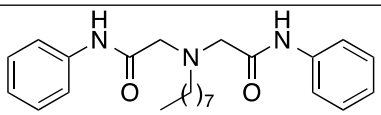	62±7
18	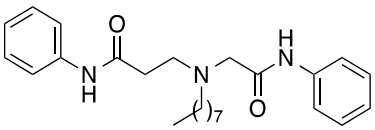	68±5
19	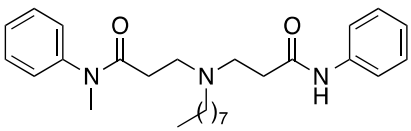	68±7

20	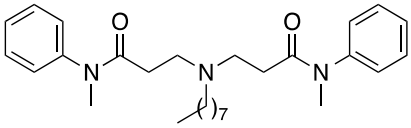	65±4
21	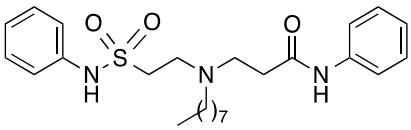	22±5
22	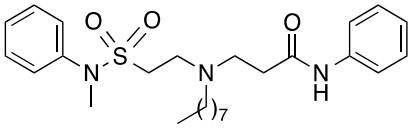	10±5
23	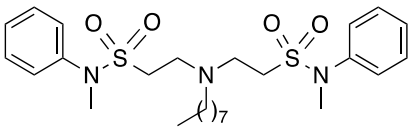	12±6
24	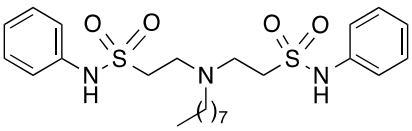	34±5

[a] The values are the mean±SEM from two to three independent experiments performed in triplicate. ICMT inhibition values were determined at 50 μM.

Table 4. Inhibition of ICMT activity of synthesized compounds **25-34**

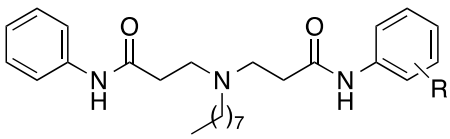

Cpd	R	ICMT inhibition (%)[a]	Cpd	R	ICMT inhibition (%)[a]
25	*o*-F	23±5	**30**	*p*-CF_3	63±7

26	*m*-F	23±4	**31**	*p*-NHCOCH$_3$	40±5
27	*p*-F	84±7 (3±1)[b]	**32**	*p*-CN	68±3
28	*o*-CF$_3$	30±6	**33**	*p*-OCH$_3$	53±4
29	*m*-CF$_3$	35±4	**34**	*p*-CON(CH$_3$)$_2$	47±5

[a] The values are the mean±SEM from two to three independent experiments performed in triplicate. ICMT inhibition values were determined at 50 μM. [b] IC$_{50}$ values for ICMT inhibition are shown between parentheses. Data correspond to the mean±SEM from two independent experiments carried out in duplicate.

Table 5. Selected data for compounds **3**, **5**, and **27**

Cpd	**ICMT inhibition (%)[a]**	**clogP[c]**	**Cellular cytotoxicity (IC$_{50}$, μM)[d]**	**Permeability (%)[e]**	**Mouse serum t$_{1/2}$ (min)[f]**	**Human serum t$_{1/2}$ (h)[f]**	**HSA binding[g] F$_b$ (K_d, μM)**
3	93±4 (2±1)[b]	4.1	5.0±0.7	68±9	171±23	>24	95.4 (28)
5	82±3 (12±3)[b]	5.1	29.1±0.6	50±3	118±17	>24	99.5 (3)
27	84±7 (3±1)[b]	4.5	13.7±0.1	54±13	55±24	>24	98.7 (7.8)

[a] The values are the mean±SEM from two to three independent experiments performed in triplicate. ICMT inhibition values were determined at 50 μM. [b] IC$_{50}$ values for ICMT inhibition are shown between parentheses. Data correspond to the mean±SEM from two independent experiments carried out in duplicate. [c] clogP values were calculated with ACDLabs Percepta Software (ACDlogP classic algorithm, version 2018.1.1). [d] Cellular viability was determined in MDA-MB-231 cells by the MTT assay. In all cases, the percentage of viable cells after treatment with 50 μM of the compound compared to vehicle was less than 5%. Data for IC$_{50}$ values correspond to the mean±SEM from at least two independent experiments carried out in duplicate. [e] Permeability is expressed as the percentage of the compound that passes through a parallel artificial membrane. Data correspond to the mean±SEM from at least two

independent experiments carried out in duplicate. [f] Data correspond to the mean±SEM from two or three independent experiments carried out in duplicate. [g] Binding to human serum albumin (HSA) is expressed as the bound fraction (F_b). Dissociation constants (K_d) are given between parentheses. Data represent the means from two independent experiments performed in duplicate. SEM is in all cases within a 10% of the mean value.

Compound 3 induces mislocalization of endogenous Ras, decreases Ras activation and induces cell death by autophagy and apoptosis

First, we checked the ability of compound **3** to produce mislocalization of endogenous Ras in PC-3 cells, which were chosen because they have high levels of ICMT and they have been described to be cysmethynil-sensitive,[30] although the direct effect of ICMT inhibition in endogenous Ras has not been ever studied. Remarkably, treatment of PC-3 cells with 5 μM of compound **3** induced significant Ras mislocalization (Figure 4). The observed effects were dose-dependent (Supporting Figure S4) and higher than the ones induced by the same concentration of cysmethynil (Figure 4 and Supporting Figure S4).

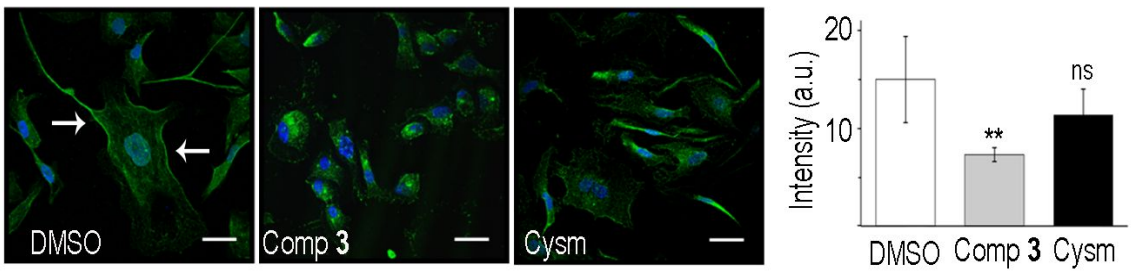

Figure 4. Compound 3 induces Ras mislocalization. Compound **3** (5 μM) induces Ras mislocalization from the cellular membrane (left image, white arrows) to intracellular locations in PC-3 cells in higher extent that cysmethynil (Cysm) at the same concentration. Immunofluorescence images show Ras in green stained using an anti-Ras primary antibody followed by the appropriate secondary FITC-labelled antibody. Nuclei (in blue) were stained with Hoechst 33258. Images were obtained in a Leica confocal microscope under the same conditions and are representative of 3 to 5 independent experiments. Bars, 30 μm. The bar graphs represent the optical density of the membrane Ras signal quantified with ImageJ. White bar, DMSO; grey bar, compound **3** (5 μM); black bar, cysmethynil (Cysm, 5 μM). Data correspond to the average±SEM of 3 independent experiments and have been analysed with GraphPad Prism 5. ns, not significant; **, P<0.01 vs DMSO (1-way ANOVA followed by the Dunnett's Multiple Comparison Test).

Importantly, Ras mislocalization paralleled substantial decreases in active Ras (GTP-bound complex) and in the activity of its downstream MEK/ERK and PI3K/AKT signalling pathways (Figure 5). These effects led finally to cellular death by autophagy, as indicated by the increase of the levels of microtubule-associated protein 1A/1B-light chain 3 (LC3), and apoptosis, as shown by the caspase-mediated cleavage of poly (ADP-ribose) polymerase (PARP) that leads to the appearance of the specific 89 kDa fragment and by the increase in the caspase 3 activity (Figure 6). Again, compound **3** induced superior effects than

cysmethynil even when used at a lower concentration (10 μM and 25 μM, respectively, Figure 6).

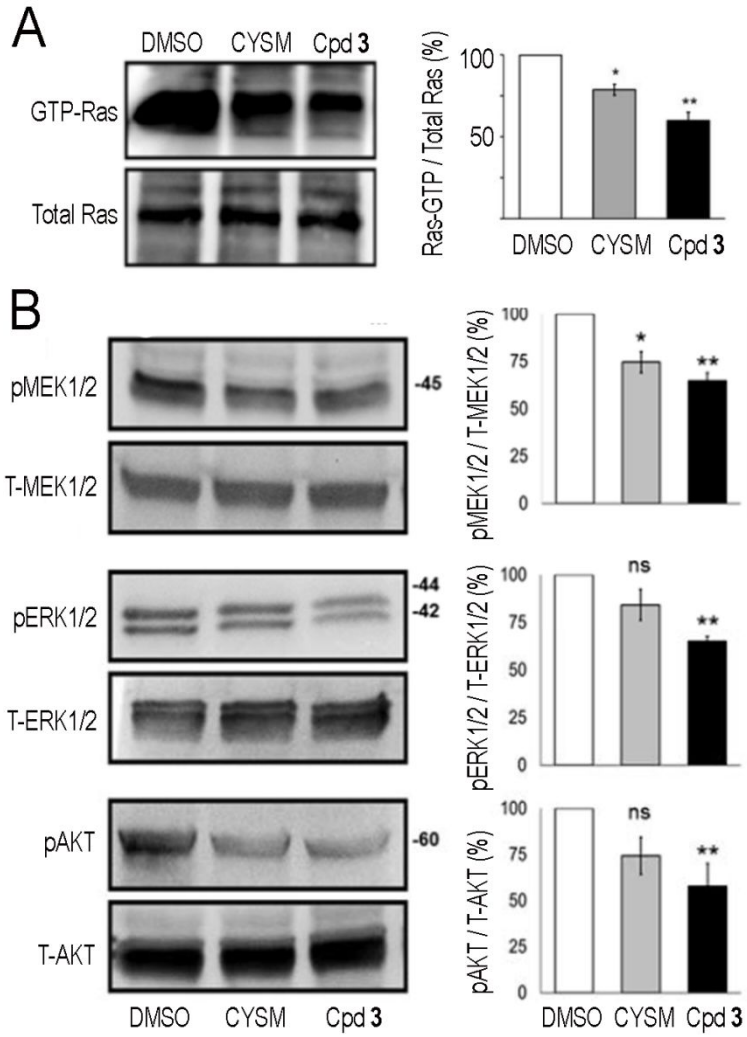

Figure 5. Compound 3 significantly reduces the Ras-GTP (active form) levels and its downstream MEK/ERK and PI3K/AKT signaling pathways. (A) Ras-GTP complex from PC-3 cells treated with DMSO, cysmethynil (CYSM, 25 μM) or compound **3** (10 μM) were immunoprecipitated and visualized by western blot. The bar graph shows the ratio Ras-GTP/total Ras, expressed as percentage relative to DMSO. (B) Representative western blots of phosphorylated MEK1/2 (pMEK1/2), ERK1/2 (p-

ERK1/2), and AKT (p-AKT) and the corresponding total kinases (T-MEK1/2, T-ERK1/2, and T-AKT). Lysates were obtained from PC-3 cells treated with DMSO, cysmethynil (CYSM, 25 μM) or compound **3** (10 μM). The bar graphs represent the optical density of the immunoreactive phosphorylated protein normalised to the total corresponding protein, and expressed as the percentage relative to DMSO. White bars, DMSO; grey bars, cysmethynil (CYSM, 25 μM); black bars, compound **3** (10 μM). Data correspond to the average±SEM of 3 to 5 independent experiments. ns, not significant; *, P<0.05; **, P<0.01 vs DMSO (Student's t test).

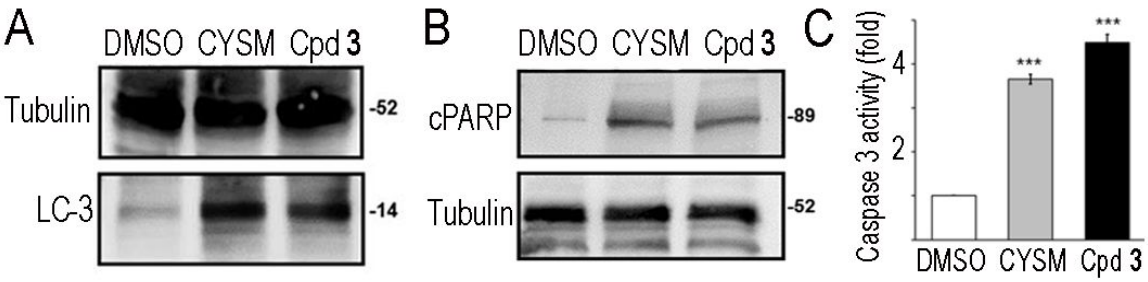

Figure 6. Compound 3 induces autophagy and apoptosis in PC-3 cells. Cells treated with DMSO, cysmethynil (CYSM, 25 μM) or compound **3** (10 μM) were lysed and stained for (A) LC-3 expression; (B) PARP levels; and (C) caspase 3 activity. Images are representative of at least three independent experiments and data in C correspond to the average±SEM of three independent experiments. ***, P<0.001 vs DMSO (Student's t test).

Compound 3 induces mislocalization of the four Ras isoforms

The four Ras isoforms (H-Ras, K-Ras4A and 4B, and N-Ras) contribute in different extent to different tumors.[31] For instance, K-Ras is the most frequently mutated isoform in the majority of cancers, with 90% of pancreatic or 35% of colon tumours harbouring K-Ras mutations. Instead, N-Ras mutations have a higher presence in melanoma and hematopoietic tumors.[32, 33] Then, it is essential to assess whether a compound affects to all the Ras isoforms. Notably, compound **3** induces the mislocalization of the four Ras isoforms (Figure 7), as shown when AD-293 cells were transfected with H-, N-, and K-Ras4A and 4B isoforms. These effects are especially significant in the case of H-Ras (most common isoform in cervix and urinary tract tumors) and K-Ras4A (necessary for lung tumor initiation),[33] where compound **3** is clearly more efficacious than the same concentration of cysmethynil.

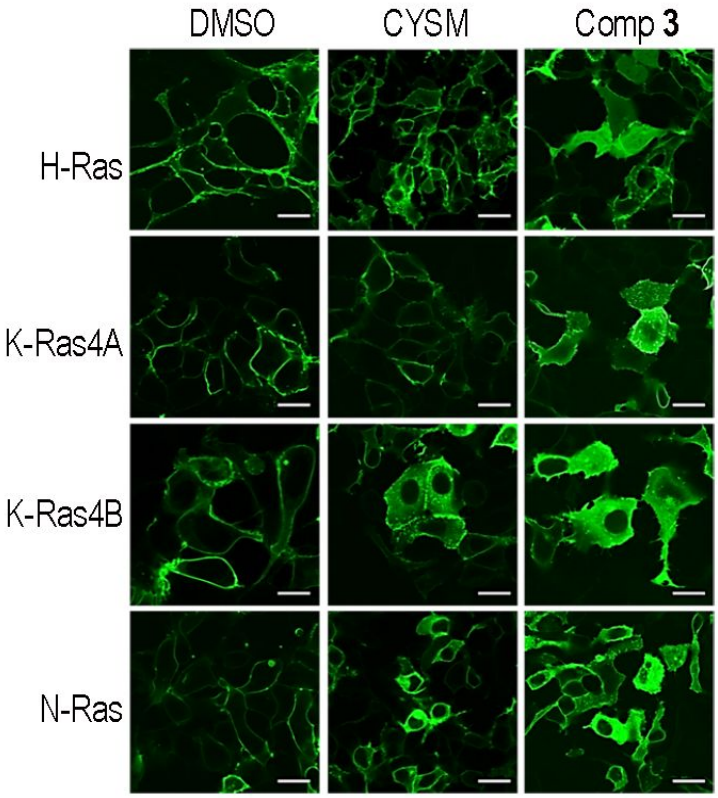

Figure 7. Compound 3 impairs plasma localization of the four Ras isoforms. Confocal images of live AD-293 cells that had been transiently transfected with H-Ras, K-Ras4A, K-Ras4B, and N-Ras GFP fusion plasmids, and treated overnight with vehicle (DMSO), cysmethynil (CYSM, 5 μM), or compound **3** (5 μM). Live cells were imaged with an inverted Zeiss LSM 510 Meta laser scanning confocal microscope. Similar results were obtained with three independent transfections performed in triplicate. Bars, 10 μm.

In order to corroborate that the observed mislocalization of the Ras isoforms is caused by ICMT inhibition, and not by other non-specific mechanisms, we corrobated that Fyn, a protein which belongs to the Src family of tyrosine protein kinases that is located at the plasma membrane after myristoylation and

palmitoylation processes, but which is not a substrate of ICMT, is not affected by compound **3** nor cysmethynil (Supporting Figure S5). We also confirmed that compound **3** did not affect geranylgeranylated proteins, because AAX removal and subsequent methylation by ICMT takes place only for formerly farnesylated Ras. The differential substrate recognition of FTase against GGTase I is dictated by the amino acid situated in the X position of the CAAX tetrapeptide: S and M defines farnesylation whereas L indicates geranylgeranylation.[34] Using a K-Ras4B protein tagged with GFP which contains a point mutation in the CAAX motif designed to replace farnesylation by geranylgeranylation, we determined the influence of compound **3**. Consistent with an ICMT-dependent effect, geranylgeranylated K-Ras4B (K-Ras4B-CVIL-GFP) was located in the plasma membrane with an identical pattern in the presence or in the absence of derivative **3**, while farnesylated K-Ras4B-GFP was mislocalized to the cytosol after the incubation with compound **3** (Supporting Figure S6). To further verify the specificity of the compound's mechanism of action we tested its effects on cells where ICMT expression has been blocked with a specific small interfering RNA as well as on the enzymes involved in the prenylation pathway (FTase, GGTase, and Rce1). Our results show that when ICMT expression is blocked with a specific small interfering RNA, compound **3** does not induce significant cytotoxicity, suggesting that the effects observed are mainly due to ICMT inhibition (Figure 8A). Moreover, this

compound does not inhibit in a noticeable manner FTase, GGTase or Rce1 enzymes, as supported by the fact that specific substrates of these enzymes remain unaffected in the presence of compound **3**. For example, protein HDJ2 is specifically farnesylated by FTase.[35] Accordingly, lonafarnib, a selective FTase inhibitor, impairs its farnesylation as revealed by the appearance of a non-farnesylated HDJ2 band in the immunoblot (Figure 8B). Conversely, neither compound **3** nor a specific GGTase inhibitor (compound GGTI298) affect HDJ2 processing. In the case of Rap1A, a specific substrate of GGTase,[35] neither compound **3** nor lonafarnib have any influence in the geranylgeranylation of this protein whereas the specific GGTase inhibitor GGTI298 clearly inhibits its prenylation, as indicated by the appearance of the corresponding upper band (Figure 8B). Similarly, compound **3** does not affect to the hydrolysis by Rce1 of the specific peptide substrate KSKTKC(farnesyl)VI[36] (Supporting Figure S7).

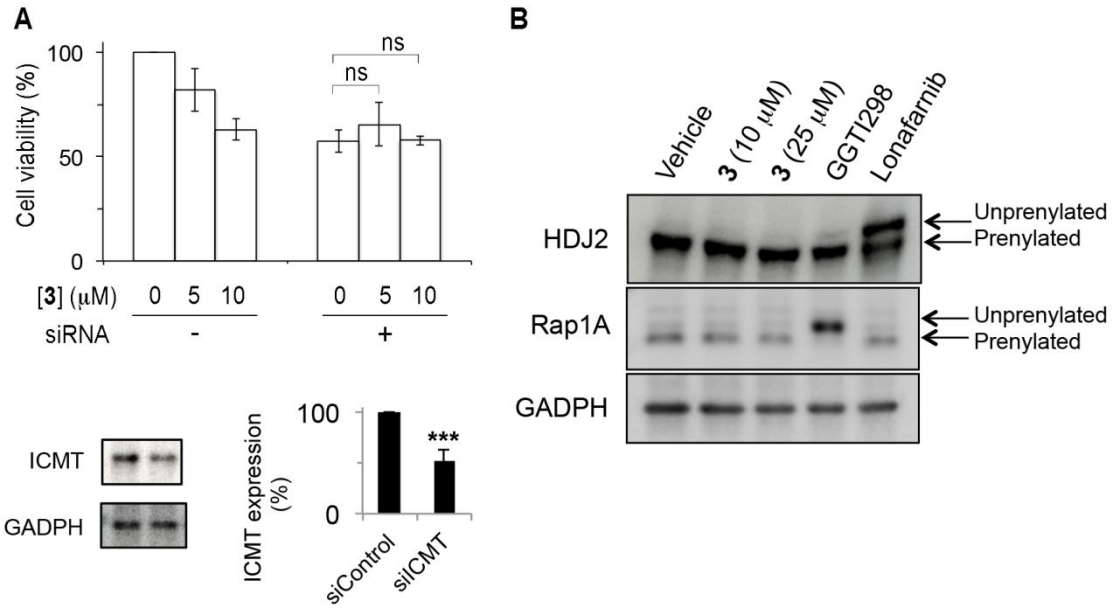

Figure 8. Compound 3 does not induce cytotoxicity in ICMT-depleted cells nor inhibits FTase or GGTase enzymes. (A) Effect of siRNA-induced silencing of ICMT gene expression on cytotoxicity induced by compound **3**. Cytotoxicity of compound **3** at different concentrations is eliminated by siRNA-induced reduction of ICMT expression levels. PC-3 cells were transfected with siRNA-targeting ICMT for 72 h. Equal amounts of total protein from PC-3 cells transfected with siRNA-targeting ICMT or with the control were subjected to immunoblotting analyses with antibodies against ICMT or GADPH as loading control. Results shown in the lower panel are the average±SEM of three different experiments. Shown gel is representative of those obtained in three independent experiments. ns, not significant; ***$p < 0.001$ (Student's t-test) vs ICMT expression in siRNA control-transfected cells. (B) Effect of compound **3** on the prenylation state of HDJ2 and Rap1A proteins. PC-3 cells were treated with

vehicle, compound **3**, GGTase inhibitor GGTI298 (10 μM) or lonafarnib (1 μM), lysed and immunoblotted with antibodies against HDJ2, Rap1A or GADPH (used as loading control). Images are representative of three independent experiments.

Compound 3 induces cell death in a variety of Ras-mutated tumor cell lines

Taken together, all these data suggest that compound **3** should be able to significantly impair cell proliferation in Ras-mutated tumor cells of different origins and with distinct Ras mutations. To assess this, we have selected a panel of cells bearing the most frequently mutated Ras isoform in the majority of cancers (K-Ras) with the most abundant point mutations (G12C, G12D, G12V, and G13D) and two cell lines with mutated N-Ras, the most important isoform in acute myeloid leukemia (AML) and in melanoma.[33] The obtained data (Table 6) show that compound **3** significantly reduces cell proliferation in all tested Ras mutant cell lines with IC_{50} values in the low micromolar range and selectivity against non-tumor fibroblasts. Although these results are consistent with a Ras-dependent cytotoxicity mediated by ICMT inhibition, the existence of genetic alterations and differences between cell lines can influence sensitivity to ICMT inhibitors and of course only a careful delineation of all the oncogenic signalling pathways together with data on ICMT expression and activity will enable the complete understanding of the ICMT contribution to cancer.

Table 6. Cytotoxicity of compound **3** in a panel of Ras-mutated cancer cell lines

Cell	Tissue Origin	Ras isoform and status	IC_{50} (μM)[a]
PANC-1	Pancreas	K-Ras (G12D)	7
MIA PaCa-2	Pancreas	K-Ras (G12C)	2
MDA-MB-231	Breast	K-Ras (G13D)	5
SW620	Colon	K-Ras (G12V)	3
SK-Mel-173	Melanoma	N-Ras (Q61K)	12
HL60	Blood	N-Ras (Q61K)	2
NIH3T3	Fibroblast	Non-tumor	> 50
142BR	Fibroblast	Non-tumor	> 50

[a]Cytotoxicity was evaluated by the MTT or the XTT assay. IC_{50} values are the means from two to three independent experiments performed in triplicate. In all cases, the SEM is within 10% of the mean value.

The dose-response analysis showed that compound **3** promoted cell death at 10 μM after 24 h treatment in MIA PaCa-2 and HuP-T4 as well as at 20 μM in the rather resistant PANC-1, PK9, and Capan-2 cell lines whereas a concentration of 50 μM was required to induce cell death with cysmethynil. Furthermore, pancreatic cancer Capan-2 cells were even resistant to this

concentration of cysmethynil (Supporting Figure S8). The analysis of the sub-G_0/G_1 region of cell cycle confirmed that compound **3** induced an apoptosis-like cell death (Supporting Figure S9).

In vivo antitumor effect of compound 3

Finally, to evaluate the potential of the ICMT inhibitor in an in vivo setting, we performed a xenograft mice model by transplanting HL-60 N-Ras mutated AML cells into NSG mice. An initial pharmacokinetic profile was carried out in mice prior to the in vivo efficacy testing. In vitro, the compound showed a half-life in mouse serum of around 3 h and in human serum of more than 24 h. For in vivo pharmacokinetic studies, mice received a single intraperitoneal injection of 25 mg/kg of compound **3** and the plasma concentration of the compound was measured at different time points (Supporting Figure S10). At this dose, concentration of compound reached a maximal concentration in serum of 1700 nM 1 h post-injection and remained around 480 nM up to 6 h post-injection, so we considered these values as satisfactory to allow the in vivo use of the compound using these conditions. Treatment of mice with compound **3** (25 mg/kg, intraperitoneally) for 15 days (3 cycles of 5 days of treatment followed by 2 days of rest) increased mice survival (Figure 9A, $p = 0.0274$) and reduced the tumor burden in the bone marrow compared with vehicle (Figure 9B,C). Before sacrifice, the serum levels of compound **3** were measured the last day of

the treatment (2 h post-injection) and turned out to be 736 nM, in full consistency with the pharmacokinetic curve. These results demonstrate the in vivo efficacy of compound **3** against Ras-dependent malignancies.

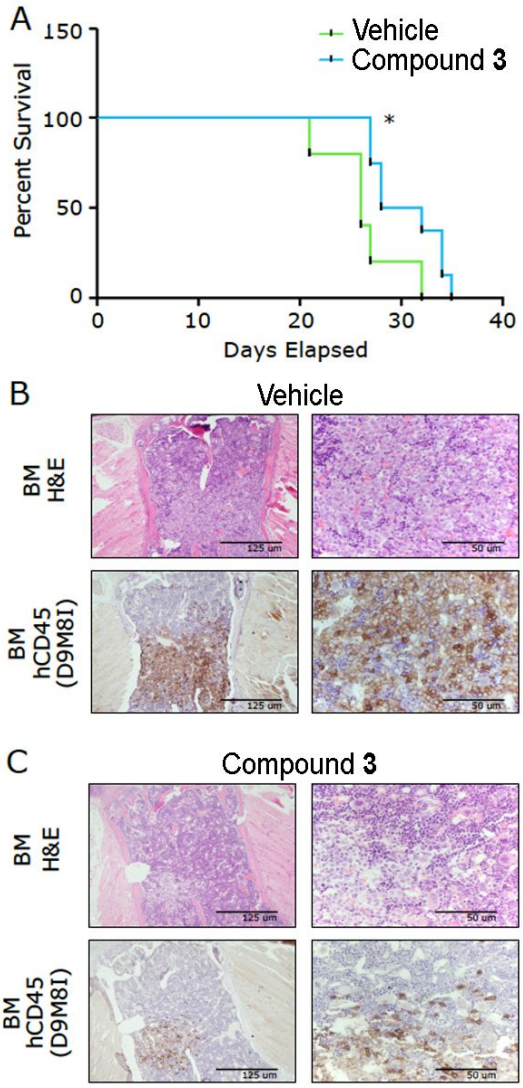

Figure 9. Antitumor effect of compound 3 in the Ras-driven model of acute myeloid leukemia. (A) Kaplan-Meier curves indicating survival of HL-60 transplanted NSG mice treated with vehicle (n=5) or with compound **3** (n=9). Statistical significance

was determined by the log rank test (p=0.0274; HR: 6.211; 95% CI or ratio: 1.225 to 31.48). Haematoxylin and eosin (H&E) and human HL-60 staining (hCD45) of paraffin-embedded bone marrow (BM) sections from wild-type HL-60 transplanted NSG mice treated with (B) vehicle or (C) compound **3**. Scale bar represents 125 μm (left images) and 50 μm (right images).

CONCLUSIONS

In this work we describe a new potent ICMT inhibitor, compound **3**,[37] that produces the mislocalization of the four Ras isoforms blocking their activation and their oncogenic signaling, leading to significant cell death in a broad panel of cell lines bearing mutated Ras and to an increased survival in the Ras-dependent cancer model of acute myeloid leukemia. These results provide strong support to the hypothesis that inhibition of the post-translational modification of Ras can be clinically relevant in Ras-driven cancers.

EXPERIMENTAL SECTION

Compound synthesis. Unless stated otherwise, starting materials, reagents and solvents were purchased as high-grade commercial products from Abcr, Acros, Fluorochem, Scharlab, Sigma-Aldrich, Honeywell, Thermo Fisher Scientific, and were used without further purification. Tetrahydrofuran (THF) and dichloromethane (DCM) were dried using a Pure SolvTM Micro 100 Liter solvent purification system. Triethylamine and pyridine were dried over KOH and distilled over CaH_2 before using.

Reactions were monitored by analytical thin-layer chromatography (TLC) on plates supplied by Merck silica gel plates (Kieselgel 60 F-254) with detection by UV light (254 nm), ninhydrin solution, or 10% phosphomolybdic acid solution in EtOH. Flash chromatography was performed on a Varian 971-FP flash purification system using silica gel cartridges (Varian, particle size 50 μm). Melting points (mp) are uncorrected and were determined on a Stuart Scientific electrothermal apparatus. Infrared (IR) spectra were measured on a Bruker Tensor 27 instrument equipped with an attenuated total reflectance (ATR) Specac accessory with diamond crystal and a transmission range of 5200-650 cm^{-1}; frequencies (υ) are expressed in cm^{-1}. NMR spectra were recorded on a Bruker Avance 300-AM (^{1}H, 300 MHz; ^{13}C, 75 MHz) at the NMR facilities of the Universidad Complutense of Madrid (UCM). Chemical shifts (δ) are expressed in parts per million relative to internal tetramethylsilane; coupling constants (*J*) are in hertz (Hz). The following abbreviations are used to describe peak patterns when appropriate: s (singlet), d (doublet), t (triplet), qt (quintet), m (multiplet), app (apparent), br (broad). NMR experiments -homonuclear correlation spectroscopy (H,H-COSY), heteronuclear multiple quantum correlation (HMQC) and heteronuclear multiple bond correlation (HMBC)- of representative compounds were acquired to assign protons and carbons of new structures. High resolution mass spectrometry (HRMS) was carried out on a FTMS Bruker APEX Q IV spectrometer in electrospray ionization (ESI) mode at

the UCM's facilities. HPLC-MS analysis was performed using an Agilent 1200LC-MSD VL. LC separation was achieved with an Eclipse XDB-C18 column (5 μm, 4.6 mm x 150 mm) together with a guard column (5 μm, 4.6 mm x 12.5 mm). The gradient mobile phases consisted of A (95:5 water/methanol) and B (5:95 water/methanol) with 0.1% ammonium hydroxide and 0.1% formic acid as the solvent modifiers. MS analysis was performed with an ESI source. The capillary voltage was set to 3.0 kV and the fragmentor voltage was set at 70 eV. The drying gas temperature was 350 ºC, the drying gas flow was 10 L/min, and the nebulizer pressure was 20 psi. Spectra were acquired in positive and negative ionization mode from 100 to 1000 m/z and in UV-mode at four different wavelengths (210, 230, 254, and 280 nm).

Spectroscopic data of all described compounds were consistent with the proposed structures. Satisfactory chromatograms were obtained for all tested compounds, which confirmed a purity of at least 95%. The synthesis and structural characterization of derivative **3** is detailed below. Full details regarding the synthetic procedures and characterization data of all compounds are given in the Supporting Information.

Synthesis of N^3-(3-Anilino-3-oxopropyl)-N^3-octyl-N^1-phenyl-β-alaninamide (3). To a solution of *N*-phenylacrylamide (500 mg, 3.4 mmol) and octylamine (182 μL, 1.1 mmol) in dry acetonitrile (1 mL/mmol of amine), DBU (508 μL, 3.4 mmol) was added at rt and under an argon atmosphere. The reaction mixture

was stirred at reflux for 16 h. The solvent was evaporated under reduced pressure and the residue was purified by column chromatography (hexane/EtOAc, 1:1) to yield compound **3** as an oil (387 mg) in 83% yield. R_f (EtOAc/MeOH, 9:1): 0.42. IR (ATR, ν): 3294 (NH), 1659, 1546 (CON), 1601, 1497 cm^{-1} (Ar). ^1H NMR ($CDCl_3$, δ): 0.85 (t, *J* = 6.7 Hz, 3H, CH_3), 1.19-1.25 (m, 10H, $(C\underline{H}_2)_5CH_3$), 1.53 (m, 2H, $C\underline{H}_2(CH_2)_5CH_3$), 2.53 (t, *J* = 6.3 Hz, 6H, $2CH_2CO$, $(CH_2)_6C\underline{H}_2N$), 2.86 (t, *J* = 6.2 Hz, 4H, $2COCH_2C\underline{H}_2N$), 7.03 (t, *J* = 7.3 Hz, 2H, $2H_4$), 7.20 (t, *J* = 7.8 Hz, 4H, $2H_3$, $2H_5$), 7.43 (d, *J* = 7.8 Hz, 4H, $2H_2$, $2H_6$), 8.91 ppm (br s, 2H, 2NH). ^{13}C NMR ($CDCl_3$, δ): 14.2 (CH_3), 22.7, 26.9, 27.8, 29.4, 29.6, 31.9 ($(\underline{C}H_2)_6CH_3$), 34.6 ($2\underline{C}H_2CO$), 50.0 ($2CH_2N$), 53.8 ($(CH_2)_6C\underline{H}_2N$), 120.0 ($2C_2$, $2C_6$), 124.1 ($2C_4$), 129.0 ($2C_3$, $2C_5$), 138.2 ($2C_1$), 170.6 ppm (2CO). MS (ESI): 424.3 [$(M+H)^+$]. HPLC-MS, t_r (min): 18.55. HRMS (ESI): calcd. for $C_{26}H_{38}N_3O_2$ [$(M+H)^+$]: 424.2958; found: 424.2958.

Determination of ICMT activity. Synthesized compounds were tested for their ability to inhibit human ICMT activity using Sf9 membranes containing the recombinantly expressed enzyme. In this assay, a mixture of biotin-farnesyl-L-cysteine and tritiated S-adenosylmethionine in the presence or absence of the compound under study was prepared and the reaction was initiated by the addition of the Sf9 membrane homogenates. The inhibitory capacity of the compounds is expressed as percentage of inhibition of the methyl esterification step, in which the tritiated methyl group of the methyl donor S-

adenosylmethionine is transferred to the substrate biotin-farnesyl-L-cysteine as described previously[13] and the radioactivity incorporated is quantified.

Cell lines and culture. MDA-MB-231, MIA PaCa-2, PANC-1, SW620, Capan-2 and NIH3T3 cells from American Type Culture Collection (ATCC, Rockville, MD) and SK-Mel-173 from Memorial Sloan-Kettering Cancer Center (New York, USA) were grown in Dulbecco's Modified Eagle medium (DMEM, Invitrogen) supplemented with 10% heat-inactivated fetal bovine serum (FBS, HyClone), 1% L-glutamine (Invitrogen), 1% sodium pyruvate (Invitrogen), 50 U/ mL penicillin and 50 μg/ mL streptomycin (Invitrogen). Human fibroblasts 142BR were from Sigma and were cultured as indicated by the vendor. Human prostate cancer PC3 cells, obtained from ATCC, and human pancreatic PK-9 cells, kindly provided by Dr. Aimable Nahimana (Lausanne, Switzerland), were maintained in Roswell Park Memorial Institute medium (RPMI) supplemented with 10% heat-inactivated FBS, 1% L-glutamine, 1% sodium pyruvate, 50 U/mL penicillin and 50 μg/ mL streptomycin. Cells were incubated at 37 ºC in the presence of 5% of CO_2. The epithelial human pancreatic adenocarcinoma cell line HuP-T4 was obtained from the European Collection of Cell Cultures (ECACC, UK) and were grown in Minimum Essential Medium Eagle's supplemented with 10% (v/v) FBS, 2 mM L-glutamine, 1 mM sodium pyruvate, 1% non-essential amino acids (GIBCO-BRL), and antibiotics.

Cell growth inhibition assay. The effect of the different compounds on the proliferation of human tumor cell lines (cytostatic activity) was determined through standard MTT or XTT assays.[3, 38, 39] For MTT assay, cells were seeded in 96-well plates at a density of 5 or 10 x 10^3 cells per well in the corresponding medium with 10% FBS for 24 h prior to treatments. The medium was then replaced by fresh medium containing different concentrations of compounds tested or by medium containing the equivalent volume of dimethylsulfoxide (DMSO, vehicle control). Cells were treated for 48 h, and then medium was replaced by fresh medium with 2 mg/mL of MTT ([3-(4,5-dimethylthiazol-2-yl)-2,5-diphenyltetrazolium bromide], Sigma-Aldrich) and cells were incubated for 4 h at 37 ºC in dark. Once supernatants were removed, formazan crystals previously formed by viable cells were dissolved in DMSO (100 μL/ well) and absorbance was measured at 570 nm (OD570-630) using an Asys UVM 340 (Biochrom Ltd., Cambridge, UK) microplate reader. Background absorbance from blank wells containing only media with compound or vehicle were substracted from each test well. Results were reported as IC_{50} ± SEM from three independent experiments.

XTT assay was carried out using the XTT (sodium 3′-[1-(phenylaminocarbonyl)-3,4-tetrazolium]-bis(4-methoxy-6-nitro)-benzenesulfonic acid hydrate) cell proliferation kit (Roche Molecular Biochemicals, Mannheim, Germany) according to the manufacturer's

instructions. Cells (0.9 × 10^3 MIA PaCa-2, 3 x 10^3 SW620, and 4 x 10_3 PANC-1 and MDA-MB-231 cells in 100 μL) were incubated in culture medium containing 10% heat-inactivated FBS in the absence and in the presence of compound **3** at different concentration ranges in 96-well flat-bottomed microtiter plates, and following 72 h of incubation at 37 °C in a humidified atmosphere of air/CO_2 (19/1), the XTT assay was performed. Measurements were performed in triplicate, and each experiment was repeated three times. The IC_{50} (50% inhibitory concentration) value, defined as the drug concentration required to cause 50% inhibition in cellular proliferation with respect to the untreated controls, was determined. Nonlinear curves fitting the experimental data were carried out in each case.

Apoptosis assay. Quantitation of apoptotic cells was determined by flow cytometry as the percentage of cells in the sub-G_0/G_1 region (hypodiploidy) in cell-cycle analysis as previously described.[40, 41]

Immunoblot analysis. Western blot analysis was carried out as described previously.[42-44] Briefly, PC3 cells were plated at a density of 2 x 10^6 cells in 15-cm dishes and allowed to grow overnight in RPMI medium with 10% FBS. The medium was then replaced by fresh medium containing 10 μM of compound or 0.1% DMSO for vehicle control. Cells were incubated in the presence of the compounds for 24 h and 1 h before the lysis they were stimulated with FBS. Cells were washed with PBS and lysed with ice-cold RIPA buffer (50 mM Tris-

HCl at pH 7.4, 150 mM NaCl, 1% Igepal) containing protease inhibitors (Roche) and phosphatase inhibitors (Phosphatase Inhibitor Cocktail 2 and 3, Sigma-Aldrich). Lysates were clarified by centrifugation at 10000 x g for 10 min at 4 ºC and used straightaway or stored at -80 ºC. Protein concentration was measured (DC Protein Assay Kit, Bio-Rad) and samples with equal amounts of total protein were diluted into a Laemmli reducing sample buffer (Bio-Rad) and denatured at 95 ºC for 5 min. Samples were then resolved on 4-20% SDS-PAGE gels (Bio-Rad) and proteins transferred to nitrocellulose membranes (GE Healthcare, Amersham). After 1 h of incubation in a blocking buffer (10 mM Tris-HCl at pH 8.0, 150 mM NaCl, 0.05% Tween-20 (TBS-T) with 1% BSA), western immunoblotting was performed overnight at 4 ºC with rabbit anti-phospho-Akt, rabbit anti-Akt, rabbit anti-phospho-ERK1/2, rabbit anti-ERK1/2, rabbit anti-phospho-MEK1/2, rabbit anti-MEK1/2, rabbit anti-α/β tubulin (1:1000, Cell Signaling), rabbit anti-ICMT (1:200, Santa Cruz) or mouse anti-Ras (1:1000, Millipore). Next day, after three 5 min washes with TBS-T, immunoblots were exposed for 1 h either to goat anti-mouse or goat anti-rabbit IgG HRP conjugate (1:5000, Sigma-Aldrich). Protein bands were visualized using enhanced chemiluminescence detection reagents (GE Healthcare, Amersham) in a Fujifilm LAS-3000 developer (Tokyo, Japan) and quantified by densitometry using ImageJ software (NIH). Relative phosphorylation levels

from three independent experiments were represented as mean ± SEM in bar graphs.

Intracellular imaging of Ras. PC3 cells were seeded at a density of 2 x 10^4 cells per well on 12-mm coverslips previously treated with poly-D-lysine hydrobromide (Sigma-Aldrich) and grown for 24 h at 37 ºC and 5% of CO_2 in RPMI medium with 10% FBS. After this time, it was replaced with fresh medium with indicated concentrations of compounds or an equivalent volume of DMSO and cells were incubated for 120 h, replacing the medium with compounds or DMSO after the first 48 h. Cells were washed twice with PBS, fixed with 4% paraformaldehyde and permeabilized with PBS-T (PBS with 0.1% Triton X-100, Sigma-Aldrich). Incubation with primary antibody mouse anti-Ras (1:200, Thermo Scientific) in PBS with 4% normal goat serum (NGS) was performed at rt with gentle shaking for 2 h. Then cells were washed twice with PBS-T and incubated 1 h in darkness with fluorescent goat anti-mouse (1:1500, Alexa Fluor 488, Life Technologies) in PBS with 1% NGS. After this time, cells were washed again twice with PBS-T and incubated with a solution of 5 μg/ mL Hoechst (Sigma-Aldrich) in PBS for 10 min at rt to visualize cell nuclei. Finally, cells were washed again thrice with PBS-T and coverslips were carefully mounted with Immumount (Thermo Scientific). Visualization was performed using an Olympus IX83 inverted confocal microscope fitted with the appropriate excitation and emission filters and a 60X oil immersion objective.

Ras-GTP pull-down assay. PC3 cells were plated at a density of 2 x 10^6 cells in 15-cm dishes and incubated in RPMI medium with 10% FBS at 37 ºC and 5% of CO_2. After 24 h, medium was replaced by fresh medium with indicated concentrations of compounds or an equivalent volume of DMSO for controls, and cells were incubated for 48 h at 37 ºC and 5% of CO_2. At this point, medium was replaced once again for fresh medium with compounds or DMSO, and the incubation was kept for other 72 h. For the analysis of active Ras (Ras-GTP), a glutathione *S*-transferase fusion of the Ras Binding Domain (RBD) of Raf1 along with glutathione (GSH) agarose resin was used (Active Ras Pull-Down and Detection Kit, Thermo Scientific). After treatments, cells were washed with PBS and lysed with ice-cold lysis buffer supplied by manufacturer. Lysates were clarified by 15 min of centrifugation at 16000*g* and protein concentration was measured using bicinchoninic acid method (Pierce BCA Protein Assay Kit, Thermo Scientific). Before performing the pull-down assay, 50 μL of each lysate were separated to analyze the total Ras expression. Equal amounts of protein from each condition were then used to carry out the pull-down assay, following manufacturer's instructions. The entire samples obtained after the pull-down assay were boiled 5 min and loaded onto 4-20% SDS-PAGE gels (Bio-Rad). Ras proteins were visualized by immunoblotting on nitrocellulose membranes using mouse anti-Ras provided by manufacturer. Blots were analyzed by

densitometry using ImageJ software (NIH). Data were representative of three independent experiments ± SEM.

RNA interference-mediated silencing of the ICMT gene. PC-3 cells were transfected with an ICMT siRNA (h) or with a control siRNA commercially available from Santa Cruz Biotechnology (sc-88830 and sc-37007, respectively), using lipofectamine and following the manufacturer's instructions. Inhibition of ICMT expression was checked by immunoblotting. To determine cytotoxicity in transfected cells, the MTT protocol indicated above was followed.

Inhibition of FTase, GGTase, and Rce1 enzymes. For FTase and GGTase, PC3 cells were treated with compound **3** or vehicle for 48 h and then lysed in Laemmli buffer (Cat. Number 161/0747, Biorad) containing protease inhibitors (protease inhibitor cocktail from Roche plus 1 mM PMSF) and phosphatase inhibitors (10 mM sodium fluoride, 0.3 μg/mL calyculin A, 1 mM sodium orthovanadate, and 10 mM β-glycerolphosphate). Lysates were subjected to SDS-PAGE using either 10% (for HDJ2) or 15% (for Rap1A) Tris-Glycine gels and then immunoblotted using antibodies specific for HDJ2 (MA5-12748, Thermo Fisher), Rap1A (Ab sc-65; Santa Cruz Biotechnology, Santa Cruz, CA), or GADPH (2118, Cell Signalling). Blots were developed using the corresponding secondary antibody and analysed as indicated above. For Rce1 inhibition, PC-3 cells were incubated in the presence or absence of compound **3** (10 μM) for 24h. Cells were homogenized in 100 mM HEPES, pH = 7.5, 5 mM

$MgCl_2$, 0.5% NP-40 buffer and flash-frozen in liquid nitrogen and stored at -80 °C until use. Aliquots were thawed quickly at 37°C and then kept on ice until dilution into buffer just before use. Reactions were performed by incubation of 0.2 mg of PC-3 homogenates in the presence of 250 μM of the Rce1 specific peptide substrate KSKTKC(f)VI (synthetized by GenScript Biotech, Netherlands BV) for 60 min at 37 ºC. Then, reactions were stopped by adding an equal volume of ice-cold acetonitrile and kept at 4 ºC until analysis by HPLC coupled to MS/MS in the UCM's Mass Spectrometry CAI as detailed below following the signal corresponding to the M+2/2 ion.

Xenograft model and in vivo treatment. All scientific procedures with animals were conformed to EU Directive 2010/63EU and Recommendation 2007/526/EC, enforced in Spanish law under Real Decreto 53/2013. Animal protocols were approved by the local ethics committees and the Animal Protection Area of the Comunidad Autónoma de Madrid (PROEX 022/17). Experiments were conducted on 8 weeks female mice from the CNIO animal facility. For pharmacokinetic studies, compound **3** was administered intraperitoneally (25 mg/kg) and blood was collected at the selected time points post-dose (n=3 per time point) by cardiac puncture. Blood was allowed to clot at room temperature for 30 min and centrifuged at 4 ºC for 10 min at 16000*g*. The supernatant was transferred to a clean polypropylene tube and stored at -80 ºC until analysis. For analysis, a volume of cold acetonitrile was added to the

serum. The sample was incubated in an ice bath for 10 min and centrifuged at 4 ºC for 10 min at 16000*g*. The resulting organic layer was filtered through a polytetrafluoroethylene filter (0.2 µm, 13 mm diameter, Fisher Scientific) and 20 µL of the sample analysed by LC-MS/MS at the UCM's Mass Spectrometry CAI. Separation was performed using a Phenomenex Gemini 5 µm C18 110A 150x2 mm column (run time 8 min; flow 0.5 mL/min; gradient: 3.5 min 5% B – 5 min 100% B – 6 min 100% B – 8 min 5% B; Phase A: water with formic acid 0.1%; Phase B: acetonitrile). The entire LC eluent was directly introduced to an electrospray ionization (ESI) source operating in the positive ion mode for LC MS/MS analysis on a Shimadzu LCMS8030 triple quadrupole mass spectrometer coupled to UHPLC with an oven temperature of 31.5 °C. The mass spectrometer ion optics were set in the multiple reaction monitoring mode and the transition selected for quantification was 423.50 > 289.05 (CE: -21v).

C57BL/6 HL-60 AML cells were obtained from DMSZ culture collection (Braunschweig, Germany) and were cultured in RPMI with 10% FBS. Five million cells were injected into the tail veins of female NOD.Cg-Prkdc(scid)Il2rg(tm1Wjl)/SzJ (NSG) mice. One week post injection, mice were treated for 3 weeks with vehicle (DMSO) or 25 mg/kg of compound **3**. Moribund mice were sacrificed according to IACUC and CNIO guidelines under protocol PROEX 022/17.

Survival analysis. Survival analysis was performed using the Kaplan-Meier method. Differences between survival distributions were analysed using the log rank test. Hazard ratio and confidence interval was obtained by Mantel-Haenszel analysis. Statistical computations were performed using GraphPad Prism 6.0.

Pathological analysis and immunohistochemistry. Mice were euthanized and tissues were collected and fixed in 10% formalin followed by paraffin embedding. Tissue sections were processed and stained with hematoxylin and eosin and pathology evaluated. Immunohistochemistry was performed by deparaffinization followed by epitope exposure using steam and citric acid. Slides were incubated in H_2O_2, blocked for 20 min at rt, and then incubated with antibodies against hCD45 (ref. 13917, Cell Signaling Technologies, Inc., Danvers, MA, USA), protein interactions were visualized by the signal detection with a peroxidase conjugated secondary antibody (EnVision+ Dual Link, Agilent, Santa Clara, CA, 113 USA) and the DAB substrate kit (ab94665, Abcam, Cambridge, UK). Slides were counterstained with Carazzi's Hematoxylin solution (PanReac AppliChem, Ottoweg, 115 Darmstadt, Germany) before mounting in DPX Mountant (Sigma-Aldrich, St.Louis, Missouri, 116 USA).

AUTHOR INFORMATION

Corresponding Authors

*For M.L.L.-R.: phone, 34-91-3944239; email: mluzlr@ucm.es

*For S.O.-G.: phone, 34-91-3945244; e-mail: siortega@ucm.es

Author Contributions: N.I.M.-R., M.B., and F.J.O. contributed equally. The manuscript was written through contributions of all authors. All authors have given approval to the final version of the manuscript.

Notes: The authors declare no competing financial interest.

ACKNOWLEDGEMENTS

This work was supported by grants from the Spanish MINECO (SAF2016-78792-R, SAF2017-89672-R) and predoctoral fellowships from CEI Moncloa (N.I.M.-R.), MINECO (M.B. and F.J.O.) and Fundación La Caixa (A.G.). The authors thank Prof. P.J. Casey for advice in the determination of ICMT inhibition and to UCM's CAIs Cytometry and Fluorescence Microscopy and Mass Spectrometry for their assistance.

ABBREVIATIONS

AFC, *N*-acetyl-*S*-farnesyl-L-cysteine; AML, acute myeloid leukemia; FTase, farnesyltransferase; GGTase, geranylgeranyltransferase; h-ICMT, human

ICMT; HSA, human serum albumin; ICMT, isoprenylcysteine carboxylmethyltransferase; LC3, microtubule-associated protein 1A/1B-light chain 3; Ma-ICMT, ICMT from *Methanosarcina acetivorans*; PARP, poly (ADP-ribose) polymerase; Rce1, endoprotease Ras-converting enzyme 1; SAM, *S*-adenosylmethionine; SEM, standard error of the mean; Tc-ICMT, ICMT from *Tribolium castaneum*.

SUPPORTING INFORMATION

Ma- and Tc-ICMT derived homology models of h-ICMT (Figures S1 and S2), concentration-response curves for cysmethynil and compound **3** (Figure S3), effect of compound **3** on the membrane association of Ras (Figure S4) and Fyn (Figure S5) and of farnesylated and geranylgeranylated K-Ras (Figure S6), and on Rce1 enzyme (Figure S7), effect of compound **3** on the induction of apoptosis en human pancreatic cancer cells (Figures S8 and S9), and plasma concentration of compound **3** after ip injection (Figure S10), computational models, detailed synthetic procedures, characterization data of final compounds **1, 2, 4-34**, and intermediates **35-55** (pdf). Molecular formula strings (csv). Homology models of human ICMT built using the crystal structure of Ma-ICMT (PDB code: 4A2N) and of Tc-ICMT (PDB code: 5V7P), as templates. This material is available free of charge via the Internet at http://pubs.acs.org.

REFERENCES

1. Lim, S. M.; Westover, K. D.; Ficarro, S. B.; Harrison, R. A.; Choi, H. G.; Pacold, M. E.; Carrasco, M.; Hunter, J.; Kim, N. D.; Xie, T.; Sim, T.; Janne, P. A.; Meyerson, M.; Marto, J. A.; Engen, J. R.; Gray, N. S. Therapeutic targeting of oncogenic K-Ras by a covalent catalytic site inhibitor. *Angew. Chem. Int. Ed. Engl.* **2014,** 53, 199-204.

2. Marin-Ramos, N. I.; Ortega-Gutierrez, S.; Lopez-Rodriguez, M. L. Blocking Ras inhibition as an antitumor strategy. *Semin. Cancer Biol.* **2019,** 54, 91-100.

3. Marín-Ramos, N. I.; Piñar, C.; Vázquez-Villa, H.; Martín-Fontecha, M.; González, Á.; Canales, Á.; Algar, S.; Mayo, P. P.; Jiménez-Barbero, J.; Gajate, C.; Mollinedo, F.; Pardo, L.; Ortega-Gutiérrez, S.; Viso, A.; López-Rodríguez, M. L. Development of a nucleotide exchange inhibitor that impairs Ras oncogenic signaling. *Chem. Eur. J.* **2017,** 23, 1676-1685.

4. Ostrem, J. M.; Shokat, K. M. Direct small-molecule inhibitors of KRas: from structural insights to mechanism-based design. *Nat. Rev. Drug Discov.* **2016,** 15, 771-785.

5. Ryan, M. B.; Corcoran, R. B. Therapeutic strategies to target Ras-mutant cancers. *Nat. Rev. Clin. Oncol.* **2018,** 15, 709-720.

6. Sautier, B.; Nising, C. F.; Wortmann, L. Latest advances towards Ras inhibition: a medicinal chemistry perspective. *Angew. Chem. Int. Ed. Engl.* **2016,** 55, 15982-15988.

7. Wang, Y.; Kaiser, C. E.; Frett, B.; Li, H. Y. Targeting mutant KRas for anticancer therapeutics: a review of novel small molecule modulators. *J. Med. Chem.* **2013,** 56, 5219-5230.

8. Wang, M.; Casey, P. J. Protein prenylation: unique fats make their mark on biology. *Nat. Rev. Mol. Cell Biol.* **2016,** 17, 110-122.

9. Cox, A. D.; Der, C. J.; Philips, M. R. Targeting Ras membrane association: back to the future for anti-Ras drug discovery? *Clin. Cancer Res.* **2015,** 21, 1819-1827.

10. Bergo, M. O.; Gavino, B. J.; Hong, C.; Beigneux, A. P.; McMahon, M.; Casey, P. J.; Young, S. G. Inactivation of Icmt inhibits transformation by oncogenic K-Ras and B-Raf. *J. Clin. Invest.* **2004,** 113, 539-550.

11. Wahlstrom, A. M.; Cutts, B. A.; Liu, M.; Lindskog, A.; Karlsson, C.; Sjogren, A. K.; Andersson, K. M.; Young, S. G.; Bergo, M. O. Inactivating Icmt ameliorates K-Ras-induced myeloproliferative disease. *Blood* **2008,** 112, 1357-1365.

12. Lau, H. Y.; Tang, J.; Casey, P. J.; Wang, M. Isoprenylcysteine carboxylmethyltransferase is critical for malignant transformation and tumor maintenance by all Ras isoforms. *Oncogene* **2017,** 36, 3934-3942.

13. Winter-Vann, A. M.; Baron, R. A.; Wong, W.; dela Cruz, J.; York, J. D.; Gooden, D. M.; Bergo, M. O.; Young, S. G.; Toone, E. J.; Casey, P. J. A small-molecule inhibitor of isoprenylcysteine carboxyl methyltransferase with antitumor activity in cancer cells. *Proc. Natl. Acad. Sci. USA* **2005,** 102, 4336-4341.

14. Wang, M.; Hossain, M. S.; Tan, W.; Coolman, B.; Zhou, J.; Liu, S.; Casey, P. J. Inhibition of isoprenylcysteine carboxylmethyltransferase induces autophagic-dependent apoptosis and impairs tumor growth. *Oncogene* **2010,** 29, 4959-4970.

15. Manu, K. A.; Chai, T. F.; Teh, J. T.; Zhu, W. L.; Casey, P. J.; Wang, M. Inhibition of isoprenylcysteine carboxylmethyltransferase induces cell-cycle arrest and apoptosis through p21 and p21-regulated BNIP3 induction in pancreatic cancer. *Mol. Cancer Ther.* **2017,** 16, 914-923.

16. Go, M.-L.; Leow, J. L.; Gorla, S. K.; Schüller, A. P.; Wang, M.; Casey, P. J. Amino derivatives of indole as potent inhibitors of isoprenylcysteine carboxyl methyltransferase. *J. Med. Chem.* **2010,** 53, 6838-6850.

17. Butler, K. V.; Bohn, K.; Hrycyna, C. A.; Jin, J. Non-substrate based, small molecule inhibitors of the human isoprenylcysteine carboxyl methyltransferase. *MedChemComm.* **2016,** 7, 1016-1021.

18. Buchanan, M. S.; Carroll, A. R.; Fechner, G. A.; Boyle, A.; Simpson, M.; Addepalli, R.; Avery, V. M.; Forster, P. I.; Guymer, G. P.; Cheung, T.; Chen, H.; Quinn, R. J. Small-molecule inhibitors of the cancer target, isoprenylcysteine

carboxyl methyltransferase, from *Hovea parvicalyx*. *Phytochemistry* **2008,** 69, 1886-1889.

19. Buchanan, M. S.; Carroll, A. R.; Fechner, G. A.; Boyle, A.; Simpson, M.; Addepalli, R.; Avery, V. M.; Hooper, J. N.; Cheung, T.; Chen, H.; Quinn, R. J. Aplysamine 6, an alkaloidal inhibitor of Isoprenylcysteine carboxyl methyltransferase from the sponge *Pseudoceratina sp*. *J. Nat. Prod.* **2008,** 71, 1066-1067.

20. Buchanan, M. S.; Carroll, A. R.; Fechner, G. A.; Boyle, A.; Simpson, M. M.; Addepalli, R.; Avery, V. M.; Hooper, J. N.; Su, N.; Chen, H.; Quinn, R. J. Spermatinamine, the first natural product inhibitor of isoprenylcysteine carboxyl methyltransferase, a new cancer target. *Bioorg. Med. Chem. Lett.* **2007,** 17, 6860-6863.

21. Leow, J. L.; Baron, R.; Casey, P. J.; Go, M. L. Quantitative structure-activity relationship (QSAR) of indoloacetamides as inhibitors of human isoprenylcysteine carboxyl methyltransferase. *Bioorg. Med. Chem. Lett.* **2007,** 17, 1025-1032.

22. Ramanujulu, P. M.; Yang, T.; Yap, S. Q.; Wong, F. C.; Casey, P. J.; Wang, M.; Go, M. L. Functionalized indoleamines as potent, drug-like inhibitors of isoprenylcysteine carboxyl methyltransferase (ICMT). *Eur. J. Med. Chem.* **2013,** 63, 378-386.

23. Lau, H. Y.; Ramanujulu, P. M.; Guo, D.; Yang, T.; Wirawan, M.; Casey, P. J.; Go, M. L.; Wang, M. An improved isoprenylcysteine carboxylmethyltransferase inhibitor induces cancer cell death and attenuates tumor growth in vivo. *Cancer Biol. Ther.* **2014,** 15, 1280-1291.

24. Bergman, J. A.; Hahne, K.; Hrycyna, C. A.; Gibbs, R. A. Lipid and sulfur substituted prenylcysteine analogs as human Icmt inhibitors. *Bioorg. Med. Chem. Lett.* **2011,** 21, 5616-5619.

25. Bergman, J. A.; Hahne, K.; Song, J.; Hrycyna, C. A.; Gibbs, R. A. *S*-Farnesyl-thiopropionic acid triazoles as potent inhibitors of isoprenylcysteine carboxyl methyltransferase. *ACS Med. Chem. Lett.* **2012,** 3, 15-19.

26. Majmudar, J. D.; Hahne, K.; Hrycyna, C. A.; Gibbs, R. A. Probing the isoprenylcysteine carboxyl methyltransferase (Icmt) binding pocket: Sulfonamide modified farnesyl cysteine (SMFC) analogs as Icmt inhibitors. *Bioorg. Med. Chem. Lett.* **2011,** 21, 2616-2620.

27. Judd, W. R.; Slattum, P. M.; Hoang, K. C.; Bhoite, L.; Valppu, L.; Alberts, G.; Brown, B.; Roth, B.; Ostanin, K.; Huang, L.; Wettstein, D.; Richards, B.; Willardsen, J. A. Discovery and SAR of methylated tetrahydropyranyl derivatives as inhibitors of isoprenylcysteine carboxyl methyltransferase (ICMT). *J. Med. Chem.* **2011,** 54, 5031-5047.

28. Yang, J.; Kulkarni, K.; Manolaridis, I.; Zhang, Z.; Dodd, R. B.; Mas-Droux, C.; Barford, D. Mechanism of isoprenylcysteine carboxyl methylation from the

crystal structure of the integral membrane methyltransferase ICMT. *Mol. Cell* **2011,** 44, 997-1004.

29. Diver, M. M.; Pedi, L.; Koide, A.; Koide, S.; Long, S. B. Atomic structure of the eukaryotic intramembrane Ras methyltransferase ICMT. *Nature* **2018,** 553, 526-529.

30. Wang, M.; Tan, W.; Zhou, J.; Leow, J.; Go, M.; Lee, H. S.; Casey, P. J. A small molecule inhibitor of isoprenylcysteine carboxymethyltransferase induces autophagic cell death in PC3 prostate cancer cells. *J. Biol. Chem.* **2008,** 283, 18678-18684.

31. Li, S.; Balmain, A.; Counter, C. M. A model for Ras mutation patterns in cancers: finding the sweet spot. *Nat. Rev. Cancer* **2018,** 18, 767-777.

32. Prior, I. A.; Lewis, P. D.; Mattos, C. A comprehensive survey of Ras mutations in cancer. *Cancer Res.* **2012,** 72, 2457-2467.

33. Stephen, A. G.; Esposito, D.; Bagni, R. K.; McCormick, F. Dragging Ras back in the ring. *Cancer Cell* **2014,** 25, 272-281.

34. Michaelson, D.; Ali, W.; Chiu, V. K.; Bergo, M.; Silletti, J.; Wright, L.; Young, S. G.; Philips, M. Postprenylation CAAX processing is required for proper localization of Ras but not Rho GTPases. *Mol. Biol. Cell* **2005,** 16, 1606-1616.

35. Lobell, R. B.; Omer, C. A.; Abrams, M. T.; Bhimnathwala, H. G.; Brucker, M. J.; Buser, C. A.; Davide, J. P.; deSolms, S. J.; Dinsmore, C. J.; Ellis-Hutchings,

M. S.; Kral, A. M.; Liu, D.; Lumma, W. C.; Machotka, S. V.; Rands, E.; Williams, T. M.; Graham, S. L.; Hartman, G. D.; Oliff, A. I.; Heimbrook, D. C.; Kohl, N. E. Evaluation of farnesyl:protein transferase and geranylgeranyl:protein transferase inhibitor combinations in preclinical models. *Cancer Res.* **2001,** 61, 8758-8768.

36. Hollander, I.; Frommer, E.; Mallon, R. Human Ras-converting enzyme (hRCE1) endoproteolytic activity on K-ras-derived peptides. *Anal. Biochem.* **2000,** 286, 129-137.

37. López-Rodríguez, M. L.; Ortega-Gutiérrez, S.; Martín-Fontecha, M.; Balabasquer, M.; Ortega-Nogales, F. J.; Marín-Ramos, N. I. Novel inhibitors of the enzyme isoprenylcysteine carboxyl methyltransferase (ICMT). WO2014118418A1, 2014.

38. Gamo, A. M.; Gonzalez-Vera, J. A.; Rueda-Zubiaurre, A.; Alonso, D.; Vazquez-Villa, H.; Martin-Couce, L.; Palomares, O.; Lopez, J. A.; Martin-Fontecha, M.; Benhamu, B.; Lopez-Rodriguez, M. L.; Ortega-Gutierrez, S. Chemoproteomic approach to explore the target profile of GPCR ligands: Application to 5-HT_{1A} and 5-HT_6 receptors. *Chem. Eur. J.* **2016,** 22, 1313-1321.

39. Marin-Ramos, N. I.; Alonso, D.; Ortega-Gutierrez, S.; Ortega-Nogales, F. J.; Balabasquer, M.; Vazquez-Villa, H.; Andradas, C.; Blasco-Benito, S.; Perez-Gomez, E.; Canales, A.; Jimenez-Barbero, J.; Marquina, A.; Del Prado, J. M.;

Sanchez, C.; Martin-Fontecha, M.; Lopez-Rodriguez, M. L. New inhibitors of angiogenesis with antitumor activity in vivo. *J. Med. Chem.* **2015,** 58, 3757-3766.

40. Gajate, C.; Barasoain, I.; Andreu, J. M.; Mollinedo, F. Induction of apoptosis in leukemic cells by the reversible microtubule-disrupting agent 2-methoxy-5-(2',3',4'-trimethoxyphenyl)-2,4,6-cycloheptatrien-1-one: protection by Bcl-2 and Bcl-X(L) and cell cycle arrest. *Cancer Res.* **2000,** 60, 2651-2659.

41. Gajate, C.; Fonteriz, R. I.; Cabaner, C.; Alvarez-Noves, G.; Alvarez-Rodriguez, Y.; Modolell, M.; Mollinedo, F. Intracellular triggering of Fas, independently of FasL, as a new mechanism of antitumor ether lipid-induced apoptosis. *Int. J. Cancer* **2000,** 85, 674-682.

42. Hernandez-Torres, G.; Cipriano, M.; Heden, E.; Bjorklund, E.; Canales, A.; Zian, D.; Feliu, A.; Mecha, M.; Guaza, C.; Fowler, C. J.; Ortega-Gutierrez, S.; Lopez-Rodriguez, M. L. A reversible and selective inhibitor of monoacylglycerol lipase ameliorates multiple sclerosis. *Angew. Chem. Int. Ed. Engl.* **2014,** 53, 13765-13770.

43. Hernandez-Torres, G.; Enriquez-Palacios, E.; Mecha, M.; Feliu, A.; Rueda-Zubiaurre, A.; Angelina, A.; Martin-Cruz, L.; Martin-Fontecha, M.; Palomares, O.; Guaza, C.; Pena-Cabrera, E.; Lopez-Rodriguez, M. L.; Ortega-Gutierrez, S. Development of a fluorescent bodipy probe for visualization of the serotonin 5-HT1A receptor in native cells of the immune system. *Bioconjug. Chem.* **2018,** 29, 2021-2027.

44. Turrado, C.; Puig, T.; García-Cárceles, J.; Artola, M.; Benhamú, B.; Ortega-Gutiérrez, S.; Relat, J.; Oliveras, G.; Blancafort, A.; Haro, D.; Marrero, P. F.; Colomer, R.; López-Rodríguez, M. L. New synthetic inhibitors of fatty acid synthase with anticancer activity. *J. Med. Chem.* **2012,** 55, 5013-5023.

Table of Contents Graphic